

## Geochemistry of the sands of the Allier river terraces, France

S.B. Kroonenberg, M.L. Moura & A.T.J. Jonker

*Department of Soil Science and Geology, Agricultural University, P.O. Box 37, 6700 AA Wageningen, the Netherlands*

Received 13 November 1987; accepted in revised form 6 January 1988

*Key words:* major and minor elements, geochemistry, sedimentary petrography, fluvial deposits, multivariate statistics, grain size, density sorting, provenance, weathering

### Abstract

The distribution of 24 major and minor elements has been studied in 66 sand samples of different grain sizes from six terrace levels along a stretch of 40 km along the Allier river, which drains an area mainly underlain by granitic and gneissic Hercynian basement and alkalibasaltic Cenozoic volcanic rocks in the French Central Massif. The river sands show a large spread in SiO<sub>2</sub> (63–97%). Principal component analysis shows two factors, F1 composed of Ti, Mg, Fe, Mn, Ca, P, Ni, Cr, V, Sr, Nb and Zr, together with –Si, mainly elements from basaltic components, and F2 composed of K, Na, Al, Rb and Ga, mainly elements of alkalifeldspar and micas. Within single terrace levels F1 varies mainly due to lateral and downstream density sorting of basaltic rock fragments, and F2 due to increasing concentration of micas in finer-grained samples. Variations in F1 between terrace levels reflect partly uplift and erosion history, partly increasing contribution of fluviglacial basalt-rich sediment in glacial times and of basement-rich sediment in interglacial times. Weathering of basaltic components with increasing sediment age is reflected in decreasing Ca/Ti and Mg/Fe ratios with terrace height. The results show that the geochemical study of unconsolidated fluvial sands is a rapid and useful tool next to classical sedimentary petrography.

### Introduction

Whereas through classical sedimentary petrographic analysis of unconsolidated sands a great amount of piecemeal information is obtained about the composition of the heavy fractions, light fractions, opaques etc., one easily loses sight of the bulk composition of the sediments.

In igneous and metamorphic petrology whole-rock geochemistry is intensively used to trace endogenous processes and environments. The differentiation of magmas, for instance, is demonstrated in the first place by systematic changes in bulk rock chemistry, often brought about by the sinking of heavier crystals in lighter melts, which is essentially

an endogenous sedimentary process. In this paper it will be shown that geochemistry can be applied in a comparable way in unconsolidated fluvial sands to illustrate sedimentary processes such as lateral and downstream sorting of particles of different size, density and shape, long-term changes in sediment supply, and post-depositional weathering processes. Chemical analyses of sands can also be used to calculate normative source rocks for direct comparison of sand composition with gravel composition (Kroonenberg & Goslings-Nieuwebeerta, in preparation).

Knowledge of the bulk sediment composition is essential (1) to unravel the fundamentals of mixing and sorting of sediments from different sources

(Franzinelli & Potter, 1983); (2) for a quantitative study of changes in fluvial sediment fluxes due to changes in the independent variables that determine the dynamic equilibrium of the fluvial system; and (3) to quantify the absolute rock volumes involved in the cycle of uplift, weathering, erosion and deposition in sedimentary basins, subduction and magma genesis. Our study is intended to be a first step to model bulk sediment fluxes in a fluvial system as a result of climatic changes and tectonic processes.

### The Allier drainage basin and its sediments

The Allier river, the main tributary of the Loire, drains a major part of the Limagne Rift Valley, a 40 km wide, N–S oriented tectonic depression in the Hercynian crystalline basement of the Central Massif. The graben itself is filled with up to 2500 m of Oligocene marls, limestones, clays and sands. The topmost filling is a thin veneer of Plio-Pleistocene quartz-rich fluvial sands, the Bourbonnais and related Lezoux sands. Both within the graben and on the uplifted borders of the Hercynian basement extensive alkalibasaltic to trachytic volcanism has taken place from the Miocene until 6000 years ago. Large Tertiary volcanic edifices such as the Cantal and Mont Dore exist next to numerous Pleistocene and Holocene scoria cones in the Chaîne des Puys and extruded domes such as the Puy de Dôme (Fig. 1). The drainage basin considered here, with a total surface of about 6600 km<sup>2</sup>, is estimated from the geological map to be underlain for about 58% by crystalline rocks (mainly migmatitic gneisses and granites) of the basement, for 20% by soft Oligocene rocks, for 19% by basaltic rocks and for 3% by intermediate and acid volcanic rocks. Details of the geology are given by Autran & Peterlongo (1980).

Strong uplift of the Central Massif from the beginning of the Quaternary onwards, forced the Allier to incise deeply into the underlying bedrock, thereby forming a flight of at least 8 alluvial terraces, the highest of which is situated at about 140 m above river level. These terraces are numbered according to French usage from z (youngest) to s

(oldest) (Jeambrun et al., 1976; Fig. 1). Beyond the terraces extensive Late Glacial to Holocene fluvial and lacustrine sediments have been deposited in thaw lake-like basins (Kroonenberg et al., 1987b). The main purpose of this study is to relate sediment composition of the different terraces to climatic and uplift history, filtering out the effects of lateral and longitudinal sorting.

Much research has been carried out on the gravels and heavy minerals of the Allier river terraces (Van Dorsser, 1969; Rudel, 1963; Pelletier, 1971; Larue, 1979, 1982; Raynal, 1984; Pastre, 1986; Tourenq, 1986; Kroonenberg et al., 1987a). The main gravel components are of granitic-gneissic and basaltic origin. The Oligocene graben-filling sediments hardly show up in the gravels because they do not form sizeable rock fragments. However, they influence sand composition to some extent (Kroonenberg & Goslings-Nieuwebeerta, in preparation).

Main heavy minerals are augite, green and brown hornblende, olivine, micas and opaques, with little differentiation from one terrace to another. Statistical analysis of heavy mineral counts by Tourenq (1986) and SEM studies by Pastre (1986) show diminishing olivine content towards the higher terrace levels, interpreted to be due to weathering. Our study corroborates this. During our study it appeared, however, that the main heavy component of the sands are well-rounded fragments of dense alkalibasaltic lavas, with a specific gravity around 3.0. Unlike the common heavy minerals, these fragments are not restricted to any particular grain size, but are abundant in all fractions from 200 to 2000  $\mu\text{m}$ . As a result, the amount of heavy fraction in many samples is extremely high (up to about 50%) in comparison to sands from other rivers. The presence of abundant basaltic and granitic material proved to be an excellent circumstance to produce large variations in geochemistry due to sorting. In fact, a whole 'differentiation series' with SiO<sub>2</sub> contents between 63 and 97% can be demonstrated.

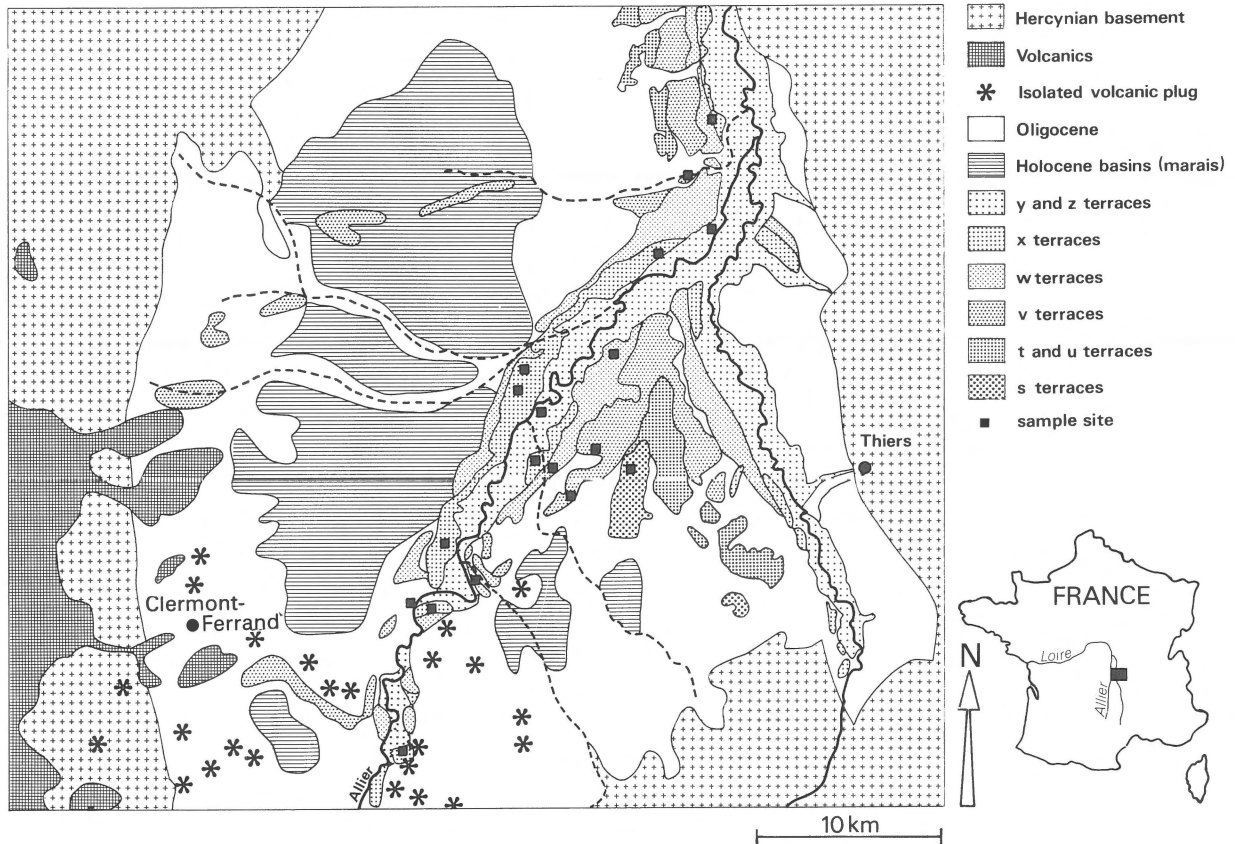


Fig. 1. Geological sketch map and sample locations.

## Materials and methods

At several sites along a stretch of 40 km along the Allier river, sand samples were taken from the present river bed (z) and from 5 different terrace levels, x, xw, w, v and s at 15, 21, 35, 60 and 100 m above river level, respectively (Fig. 2; the xw terraces are considered to be eroded remnants of the w terrace). In this part of the river, between the confluences with the Couze Chambon in the south and the Dore in the north, no major tributaries debouch into the Allier. At each sampling site 2–6 samples of different grain size distribution were collected, amounting to a total of 66 samples. In this way, three parameters were considered during sampling: terrace altitude relative to the present river bed (RELALT); upstream distance from the confluence with the major tributary Dore (UPSTREAM); and grain size (MEDIAN, determined

in the laboratory, see below). Care was taken to sample as much as possible sand from foreset laminae in small-scale cross-bedded sets, in order to avoid concentrations of heavy minerals in horizontally laminated lag deposits and to assure homogeneity of the sample set. Sampling depth was uniform as much as possible, and in all cases over 2 m to avoid the effect of soil formation.

In the laboratory, detailed granulometrical analyses were carried out (13 fractions) and the medians were determined from the cumulative frequency plots. Medians range from 160 to 1600  $\mu\text{m}$ . From part of the sample (separated with a sample splitter), organic matter, calcium carbonate, free iron and all material  $< 16 \mu\text{m}$  was removed by standard methods, in order to enable direct comparison of chemical composition with optically determinable mineralogy and to avoid the effect of accumulated secondary products. Only in excep-

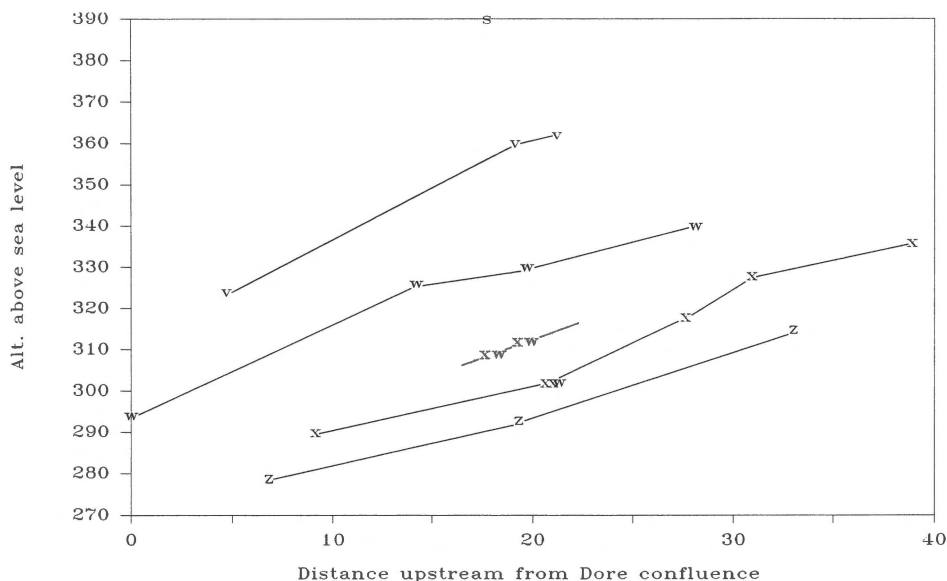


Fig. 2. Sampling sites along longitudinal terrace profiles.

tional cases the fraction  $< 16 \mu\text{m}$  amounted to more than 1% by weight of the total sample. After this pretreatment, 1 g of the sample was separated with a micro-sample splitter, fused with 2,4 lithium tetraborate and analysed for 24 major and minor elements with X-ray fluorescence spectroscopy on a Philips XRF assembly. Analysed elements are Si, Ti, Al, Fe, Mn, Mg, Ca, Na, K, P, Ba, V, Cr, Co, Ni, Cu, Zn, Ga, Rb, Zr, Nb, Sr, La and Pb. The system is calibrated using USGS geochemical standards as listed by Abbey (1980, p. 16). The results are compiled in Table 1.

### Statistical treatment of the results and its interpretation

Perusal of the results shows a large spread in the distribution of most elements between terrace levels, the most obvious being the  $\text{SiO}_2$  content, which varies from 63 to 97% by weight. (Table 1, Fig. 3a, b). For an interpretation of these data, multivariate statistical analyses were carried out, using the FACTOR, SPSS and STATPAK packages. First, a factor analysis was carried out using 23 of 24 elements (Co was excluded because contamination

during sample preparation was suspected). Factor extraction was based on principal components of the correlation matrix. The three principal factors considered (F1, F2, F3; Table 2) are responsible for 64.7, 16.6 and 4% of the total variance, respectively.

Factor scores for F1 and F2 were calculated for all samples and plotted in Fig. 4. It shows basically three clusters, differentiated mainly on account of F1. The samples from the x terrace have high negative loadings for F1, the samples from the s terraces high positive loadings for F1, whereas samples from z, xw, w and v occupy an intermediate position and are not differentiated from each other by F1. z samples have a smaller spread in F2 values than the other terrace samples in this cluster.

To evaluate the relation of the chemical composition with the parameters RELALT, MEDIAN and UPSTREAM, another factor analysis was carried out, now including those parameters. In this case only those 15 elements that showed highest overall correlation coefficients in the correlation matrix were considered. This procedure again led to the distinction of three factors F1', F2' and F3', accounting for 58.0, 18.9 and 6.2% of total variance, respectively (Table 3). The input parameter

UPSTREAM is included into F1', MEDIAN into F2' and F3' is composed of RELALT alone.

In both cases, Si has a very high loading in F1 with a sign opposite to that of the other elements. Therefore, most of the variation in F1 can be visualized by considering variation in SiO<sub>2</sub> alone. In Fig. 5 the correlation coefficients between SiO<sub>2</sub> and input variables MEDIAN and UPSTREAM are calculated *per terrace level*. They show that for all terraces except x there is also a reasonable negative correlation between MEDIAN and SiO<sub>2</sub> which was not evident from the analysis of the whole data set. Figure 6 shows the relation between SiO<sub>2</sub> and RELALT. Details about the statistical treatment of the data are available upon request.

In terms of sedimentary petrography, Factor 1 of both statistical analyses clearly includes those elements concentrated in basaltic minerals such as

augite, olivine, Fe-Ti opaques, amphiboles, next to calcic plagioclase. Factor 2 on the other hand, includes elements fractionated by alkali feldspars and micas, predominantly of crystalline provenance. Surprisingly, however, SiO<sub>2</sub> does not show a positive correlation with Factor 2 but a negative correlation with Factor 1. Therefore, Factor 2 is not simply a 'granitic' factor.

The overall relations described above can be paraphrased as follows:

1. *MEDIAN: (Variation at single sample sites by lateral sorting):* an increase of mica/alkali feldspar towards the finer fractions; a decrease of basaltic elements and concomitant increase in SiO<sub>2</sub> in the z, xw, w, v and s terraces towards coarser-grained samples, but a rather erratic behaviour in the x terrace.

2. *UPSTREAM: (Variation within single terrace*

*Table 1.* Averages and ranges of major and minor elements per terrace level. Z is the average of n analyses, Z+ the maximum value and Z- the minimum value found for the corresponding element in that particular terrace. SiO<sub>2</sub> to P<sub>2</sub>O<sub>5</sub> in weight percentages of the oxides, V to Pb in weight ppm of the elements. 0 means below detection limit.

Terrace	Z n = 12	Z-	Z+	X n=18	X-	X+	XW n = 11	XW-	XW+	W n = 12	W-	W+	V n = 10	V-	V+	S n = 3	S-	S+
SiO <sub>2</sub>	77.53	71.70	81.34	68.93	63.01	75.43	78.31	73.05	84.04	79.18	72.53	85.02	76.41	68.79	81.47	90.71	83.10	97.08
TiO <sub>2</sub>	0.57	0.37	0.90	1.25	0.85	1.78	0.55	0.35	0.79	0.41	0.19	0.71	0.63	0.27	1.39	0.11	0.03	0.24
Al <sub>2</sub> O <sub>3</sub>	11.02	9.61	13.55	12.46	11.16	15.03	10.94	7.84	12.68	11.42	9.19	15.19	11.88	9.08	15.61	5.65	2.44	9.47
Fe <sub>2</sub> O <sub>3</sub>	2.49	1.51	4.31	5.27	3.51	7.87	2.09	1.32	3.31	1.72	0.82	2.76	2.58	0.96	6.21	0.59	0.36	1.06
MnO	0.03	0.02	0.06	0.07	0.04	0.10	0.02	0.01	0.04	0.02	0.00	0.03	0.03	0.01	0.09	0.00	0.00	0.01
MgO	1.29	0.75	2.24	2.94	1.81	4.60	0.92	0.44	1.82	0.60	0.27	0.94	0.75	0.22	1.76	0.15	0.03	0.38
CaO	1.64	1.19	2.40	2.94	1.81	4.60	1.41	0.62	2.64	0.90	0.43	1.70	1.19	0.54	2.78	0.17	0.00	0.50
Na <sub>2</sub> O	2.25	1.97	2.60	2.30	2.03	2.56	2.19	1.50	2.64	2.15	1.61	3.15	2.42	1.69	3.63	0.64	0.03	1.69
K <sub>2</sub> O	2.97	2.48	3.36	2.52	1.92	3.01	3.01	2.18	3.47	3.22	2.85	3.69	3.34	2.84	3.80	2.57	1.33	3.21
P <sub>2</sub> O <sub>5</sub>	0.15	0.12	0.20	0.31	0.20	0.44	0.14	0.10	0.22	0.09	0.06	0.12	0.11	0.06	0.12	0.03	0.01	0.07
V	81	49	145	153	100	232	71	45	100	48	22	91	76	35	163	17	13	19
Cr	13	0	51	73	19	148	3	0	21	3	0	23	3	0	18	0	0	0
Co	40	27	58	36	27	50	39	24	72	41	27	59	33	8	51	50	40	62
Ni	13	2	36	43	18	82	9	0	24	4	0	12	2	0	14	0	0	0
Cu	2	0	10	13	0	35	2	0	12	1	0	5	2	0	11	0	0	0
Zn	17	0	35	47	23	76	7	0	27	5	0	32	18	0	58	0	0	0
Ga	11	8	16	13	11	16	12	10	16	11	8	14	12	10	16	7	6	7
Rb	100	82	130	98	54	187	101	64	134	124	91	218	120	83	194	102	39	166
Sr	234	198	276	388	292	531	227	178	305	214	149	375	271	184	386	88	43	131
Zr	94	61	194	161	116	215	77	53	120	76	33	212	113	50	173	38	0	101
Nb	9	6	14	15	10	21	8	6	10	8	5	16	12	8	16	3	0	7
Ba	672	579	802	673	579	785	647	506	707	715	618	879	731	570	844	613	287	889
La	13	0	46	32	0	68	12	0	37	16	0	38	20	8	30	16	0	33
Pb	12	6	29	9	0	15	12	7	17	12	6	17	12	3	19	15	6	19

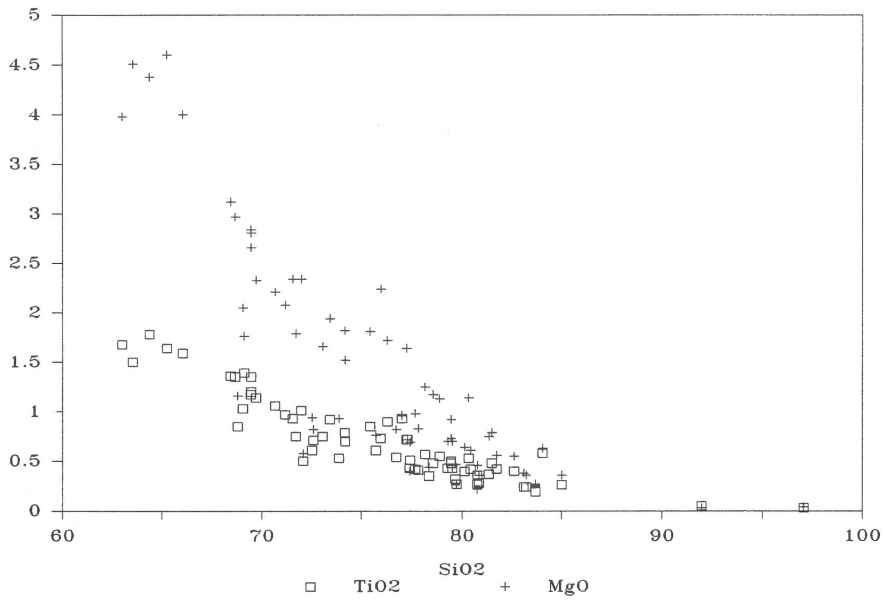


Fig. 3a. Bivariate plot of MgO and TiO<sub>2</sub> against SiO<sub>2</sub>.

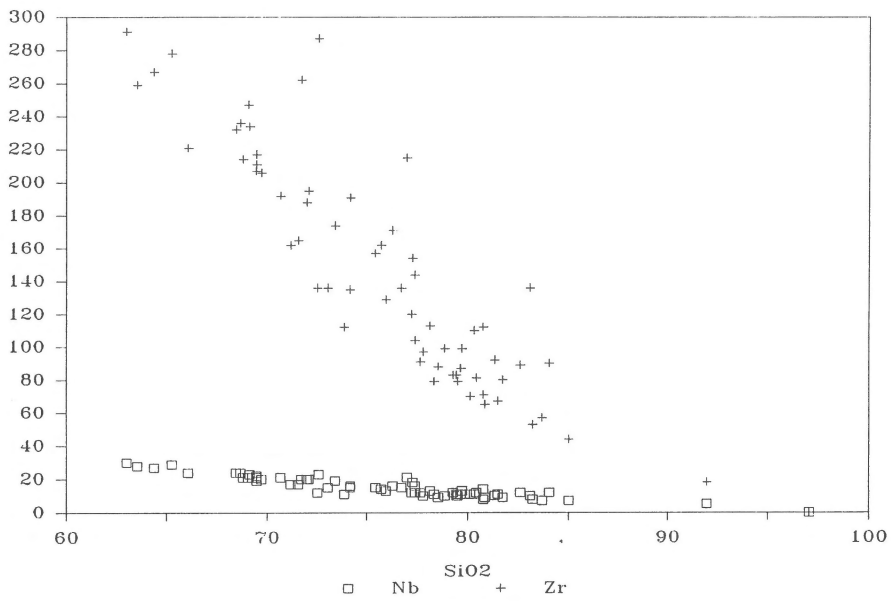


Fig. 3b. ZrO<sub>2</sub> and Nb<sub>2</sub>O<sub>5</sub> against SiO<sub>2</sub>.

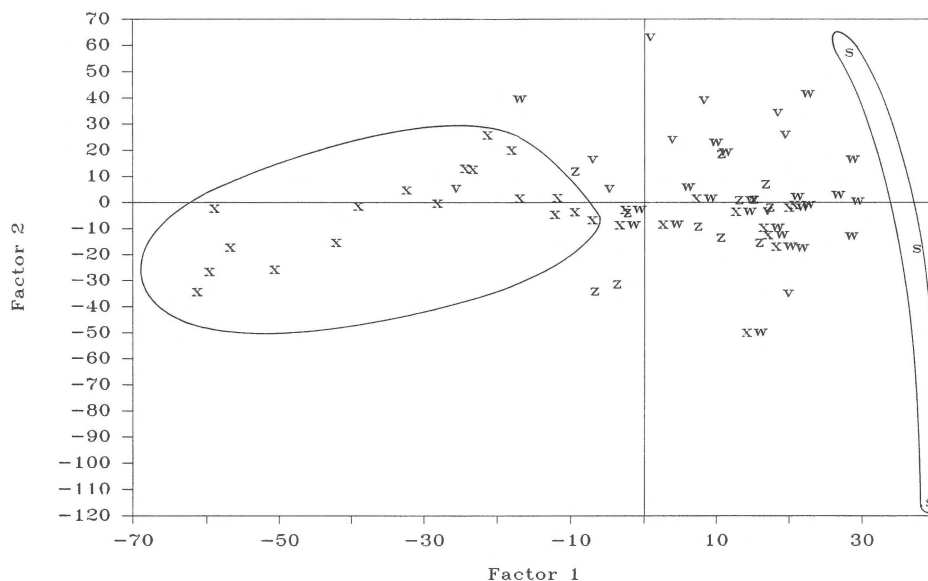


Fig. 4. Factor scores for 23 elements for all samples. Data points indicated by terrace symbols.

Table 2. Factor loadings for 23 elements (FACTOR package); F1, F2 and F3 amount to 64.7, 16.6 and 4% of total variance, respectively.

	1	2	3
Si	0.93	-0.34	0.07
Ti	-0.98	-0.07	-0.01
Al	-0.56	0.78	-0.12
Fe	-0.98	-0.07	-0.02
Mn	-0.96	-0.11	-0.02
Mg	-0.96	-0.18	0.06
Ca	-0.95	-0.17	0.07
Na	-0.37	0.82	-0.15
K	0.55	0.77	0.03
P	-0.93	-0.15	0.11
V	-0.96	-0.13	-0.03
Cr	-0.91	-0.22	0.10
Ni	-0.92	-0.22	0.08
Cu	-0.85	-0.13	0.19
Zn	-0.91	0.06	-0.06
Ga	-0.60	0.49	-0.33
Rb	0.13	0.80	-0.02
Sr	-0.93	0.12	0.07
Zr	-0.90	0.26	0.01
Nb	-0.93	0.20	0.04
Ba	0.11	0.69	0.41
La	-0.66	0.18	0.35
Pb	0.49	0.19	0.64

levels by longitudinal sorting): a general decrease of basaltic components and a  $\text{SiO}_2$  increase downstream.

3. *RELALT*: (Variation between terrace levels by long-term changes in sediment supply): a high content of basaltic components and low  $\text{SiO}_2$  in the x terrace, a very low basalt content but very high  $\text{SiO}_2$  in the s (Lezoux sands, 100 m) terrace, and intermediate values in z (present valley bottom) and xw, w, and v terraces.

#### Variation at single sampling sites: lateral sorting

As at each site several samples of different grain size were collected, at approximately the same depth, the per site variation in sediment composition largely reflects lateral sorting. As shown above, in all terraces Factor 2 elements (K, Na, Rb, Al; i.e., those elements concentrated in micas and feldspars) show a negative correlation with MEDIAN. Bivariate plots of these elements with MEDIAN show that for medians above  $500 \mu\text{m}$ , no correlation exists, but from  $500 \mu\text{m}$  downwards notably K and Rb increase with decreasing grain size

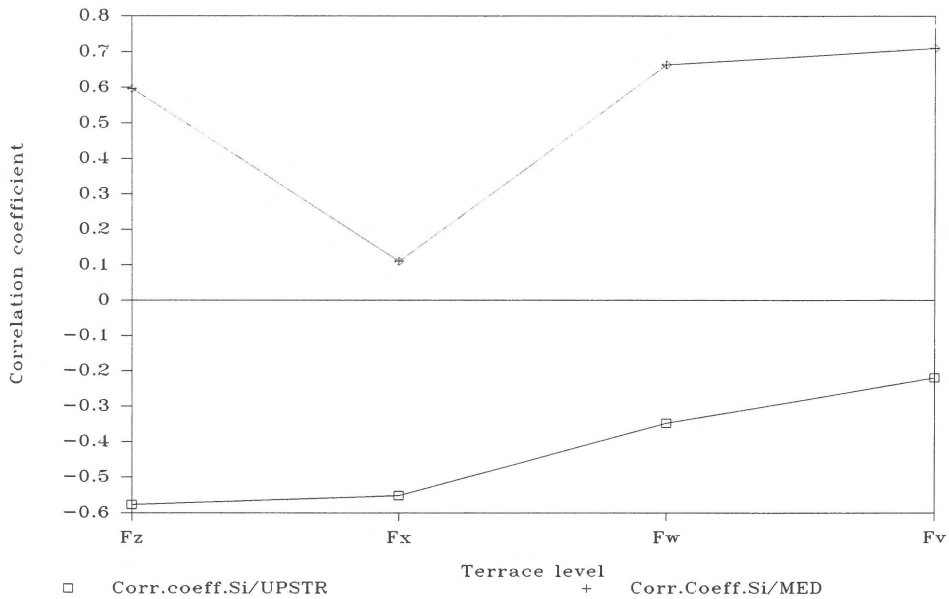


Fig. 5. Correlation coefficients for MEDIAN and UPSTREAM with SiO<sub>2</sub> per terrace level. xw and w terraces are taken together.

Table 3. Factor loadings for 15 elements and parameters RELALT, UPSTREAM and MEDIAN (SPSS package), F1', F2' and F3' amount to 58.0, 18.9 and 6.2 of total variance, respectively.

	Factor 1	Factor 2	Factor 3
TiO <sub>2</sub>	.96314		
Fe <sub>2</sub> O <sub>3</sub>	.95788		
MgO	.95198		
CaO	.94166		
SiO <sub>2</sub>	-.93942		
V	.91421		
Sr	.91420		
Zr	.88702		
Ni	.87218		
Cr	.84448		
UPSTR	.63009		
Ga	.62529	.50192	
Rb		.81589	
Na <sub>2</sub> O		.80138	
Al <sub>2</sub> O <sub>3</sub>	.60782	.76369	
MEDIAN		-.61415	
K <sub>2</sub> O	-.54827	.60611	
RELALT			.53515

(Fig. 7). This reflects increasing concentration of micas (mainly biotite) in the finer fractions, as micas fractionate Rb much more than feldspars do. If this effect were due to alkali feldspar concentration, Factor 2 should include those elements fractionated by feldspars, notably Sr and Ba, which is not the case. Concentration of micas in finer samples is also evidenced by heavy mineral counts of samples from the same site (Fig. 10, see below). Concentration of mica in the finer fractions may be attributed to sorting by shape rather than by density.

In all terraces except x, there is also a negative correlation between MEDIAN and Factor 1 ('basalt content'; Table 3, Fig. 5). This means that coarser samples have less basaltic components than finer samples. Inasmuch the maximum grain size of individual heavy minerals does not surpass 500  $\mu\text{m}$  as a rule, this trend is understandable to some extent. The lack of correlation between MEDIAN and F1 in the x terrace may be related to the fact that the heavy fractions of many samples not only contain individual mineral grains, but also large amounts of rounded fragments of basaltic lava.

In order to study the distribution of heavy parti-

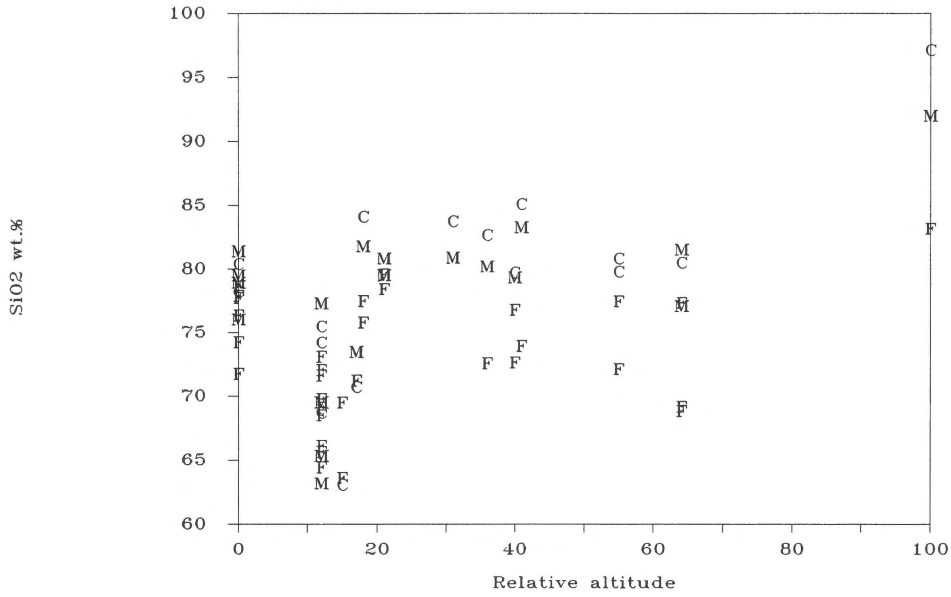


Fig. 6. Bivariate plot for SiO<sub>2</sub> and relative altitude. Data labels indicate median: C = coarse, 900–1600 μm; M = medium, 500–900 μm; F = fine, 160–500 μm).

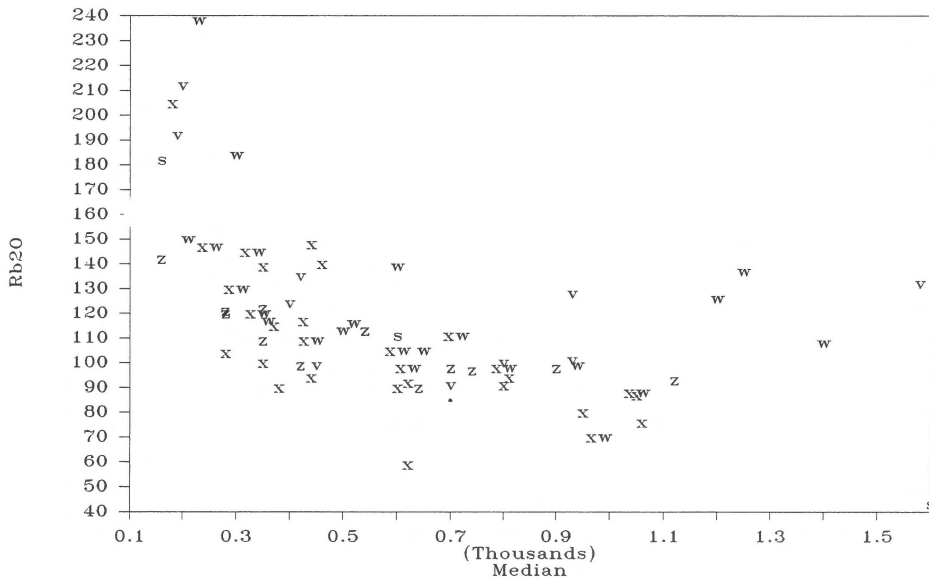


Fig. 7. Bivariate plot of Rb<sub>2</sub>O with median. Data points indicated by terrace symbols.

cles in the x terrace, two samples of different grain size from a single sand lens were first sieved into grain size fractions and then the content of heavy particles of each fraction was determined (Fig. 8). These data show that:

1. the total percentage of heavy particles is unusu-

ally high in all fractions in comparison to ordinary sands, and may even surpass 50%. It is also much higher than in sands from the other terraces (see Fig. 10 below).

2. heavy fragments are not limited in size to the < 500 μm fractions as are most individual heavy minerals in ordinary sands;

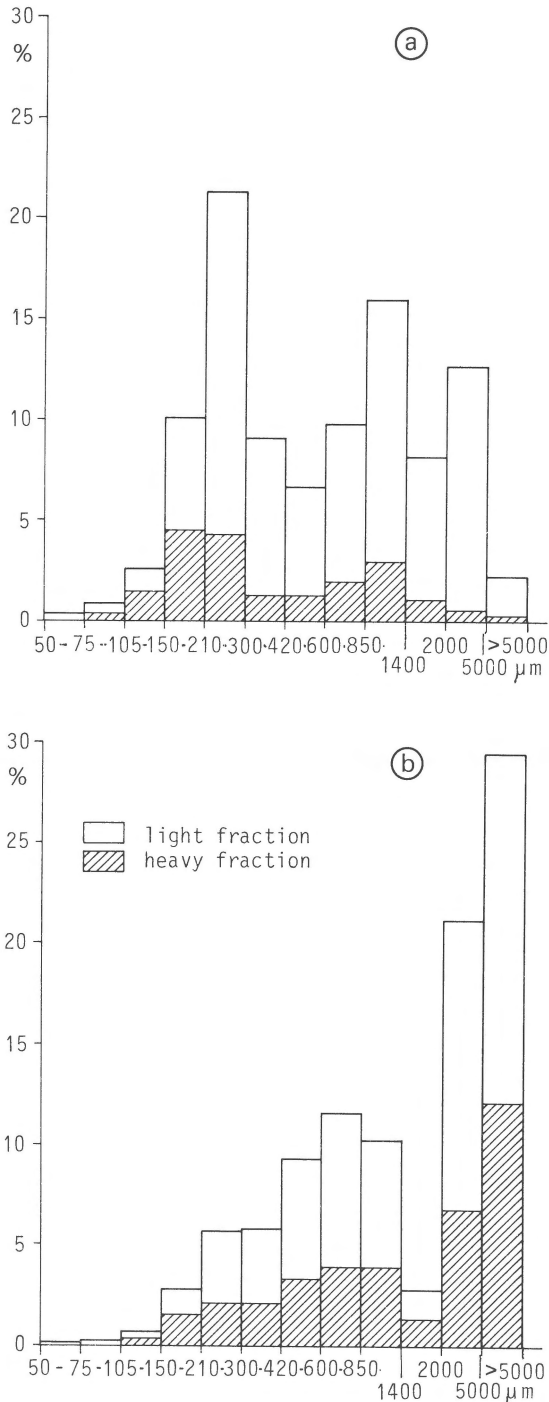


Fig. 8. Grain size distribution of two samples from the same sand lens (x terrace, Culhat quarry) with medians 380 (a) and 600  $\mu\text{m}$  (b), respectively. Hatched parts indicate percentage of heavy fragments ( $>2.89$ ) in each fraction.

3. the total percentage of heavy particles is higher in each fraction of the coarse sample than in the finer one except for grain sizes below 150  $\mu\text{m}$  (Fig. 8);
4. analysis of each heavy fraction shows that the heavy residues of the grain size fractions  $>210 \mu\text{m}$  in both the coarse and the fine sample consist mainly of basaltic rock fragments. Those of the fractions  $<210 \mu\text{m}$  consist mainly of individual mineral grains. The main difference in mineralogical composition of the individual heavy mineral grains is the concentration of micas in the finer-grained sample (cf. Fig. 10).

The negative correlation between basalt content and MEDIAN in the other terraces is mainly determined by the restriction of individual heavy mineral grains to the finer grain sizes. In the x terrace, however, heavy particles abound in all grain size fractions. The lack of correlation between basalt content and MEDIAN cannot be due to restricted availability of heavy fragments but may be attributed to the effects of density sorting.

The fundamentals of sorting of heavy minerals in fluvial sands, based on Stokes' law, have been discussed e.g. by Rubey (1933), Van AnDEL (1950) and Schuiling et al. (1985). However, field practice and experimental work show, that heavy particles rarely present the theoretical distribution predicted by Stokes' law. Partly this is due to systematic deviations caused by turbulence around sinking grains. Furthermore, the role of the original size distribution with which they were supplied to the sediment may be preponderant (Van AnDEL, 1950). Repeated reworking in sediments with particles of different density leads to concentration of coarser and heavier fragments in lag deposit and placers, often even at very specific sites in the channel such as breaks in the longitudinal profile and at river confluences (e.g., Schumm et al., 1987). In a similar way, fragments lighter than quartz such as pumice also concentrate in separate layers (Smith & Smith, 1985). Usually the percentage of heavy particles in sands is very small, and they are commonly restricted to the fine sand sizes, so concentration occurs only at particular stream velocities. Therefore, the effect of their subtraction on the bulk chemical composition of the sediment is relatively unimpor-

tant. However, in the present case, in which half of the sediment consists of heavy particles of all grain sizes, concentration in lag deposits occurs at all stream velocities, and the sediment which remains in transport is considerably enriched in lighter particles. In fact a kind of *sedimentary differentiation* occurs, not unlike magmatic differentiation. Deposition of a basalt-enriched lag deposit results in a basalt-depleted sediment load being transported further downstream. Reworking of this sediment again leads to deposition of a basaltic concentrate, thus leaving a still more basalt-depleted sediment in transport. It is believed that these longitudinal and lateral fractionation processes are responsible for the larger part of the compositional variation within terraces, and especially in the x terrace. The fact that reworking, concentration and depletion take place simultaneously in sands of all different granulometric characteristics, explains the lack of correlation between basalt content and median in this terrace.

#### **Variation within single terrace levels: longitudinal sorting**

Three or four sampling sites were selected in each terrace level along a stretch of about 40 km along which no significant tributaries debouched in the Allier river. Longitudinal variation, therefore, is mainly due to downstream sorting and differential weathering and wearing of sediment particles. As shown above, in all terraces Factor 1 (basalt content) shows a positive correlation with UPSTREAM, i.e. downstream decrease of basaltic components. This may again be explained by downstream density sorting, i.e. more traveling time for the heavier basaltic components. Selective wear of the softer basaltic particles in comparison to harder quartz and feldspar grains may also play a role, as basalt fragments are usually well-rounded, whereas feldspar and quartz grains are subrounded to subangular. Lastly, it cannot be excluded that samples downstream contain more reworked material from higher, basalt-poorer terrace levels.

#### **Variation between terrace levels: the effect of weathering**

Before being able to interpret the differences between the terrace levels, the effect of weathering must be considered. The terraces range in age from Early Pleistocene (s) to Holocene (z). Increasing weathering is evident in the field by increasing patina thickness of basaltic pebbles and increasing disintegration of coarse granite pebbles towards the higher terrace levels. Although the statistical treatment does not give direct clues to weathering, bivariate plots of specific element ratios with terrace height show notable differences. There is a marked decrease in Mg/Fe ratio and Ca/Ti ratio with terrace height, with highest values in the present river bed and lowest in the s terrace (Fig. 9a, b). The steeper slope of the Mg curve in comparison with the Ti curve in Fig. 3a reflects this as well. Several elements are depleted beyond the detection limit. The strong decrease in Mg and Ni is probably related to the virtual disappearance of olivine in the higher terrace levels (Fig. 10; cf. also Pastre, 1986; Tourenq, 1986). The decrease in Cr can be attributed to weathering of individual augite grains, as evidenced by Pastre (1986) in SEM studies, as well as of basaltic lava fragments. The lower amount of Ca probably reflects weathering of calcic plagioclase. Furthermore there is a strong increase in the amount of opaques with respect to the amount of basalt fragments and transparent minerals in the heavy fractions (Fig. 10).

This regular weathering trend is independent from the variation due to long-term changes in sediment supply (see below).

The steady decrease of the correlation coefficient between Si and UPSTREAM with increasing terrace height (Fig. 5) might also be due to weathering: Coarse-grained basaltic particles most likely do lag behind upstream, tend to disintegrate by weathering, and hence their influence on downstream compositional change by sorting is strongly diminished in the higher terraces.

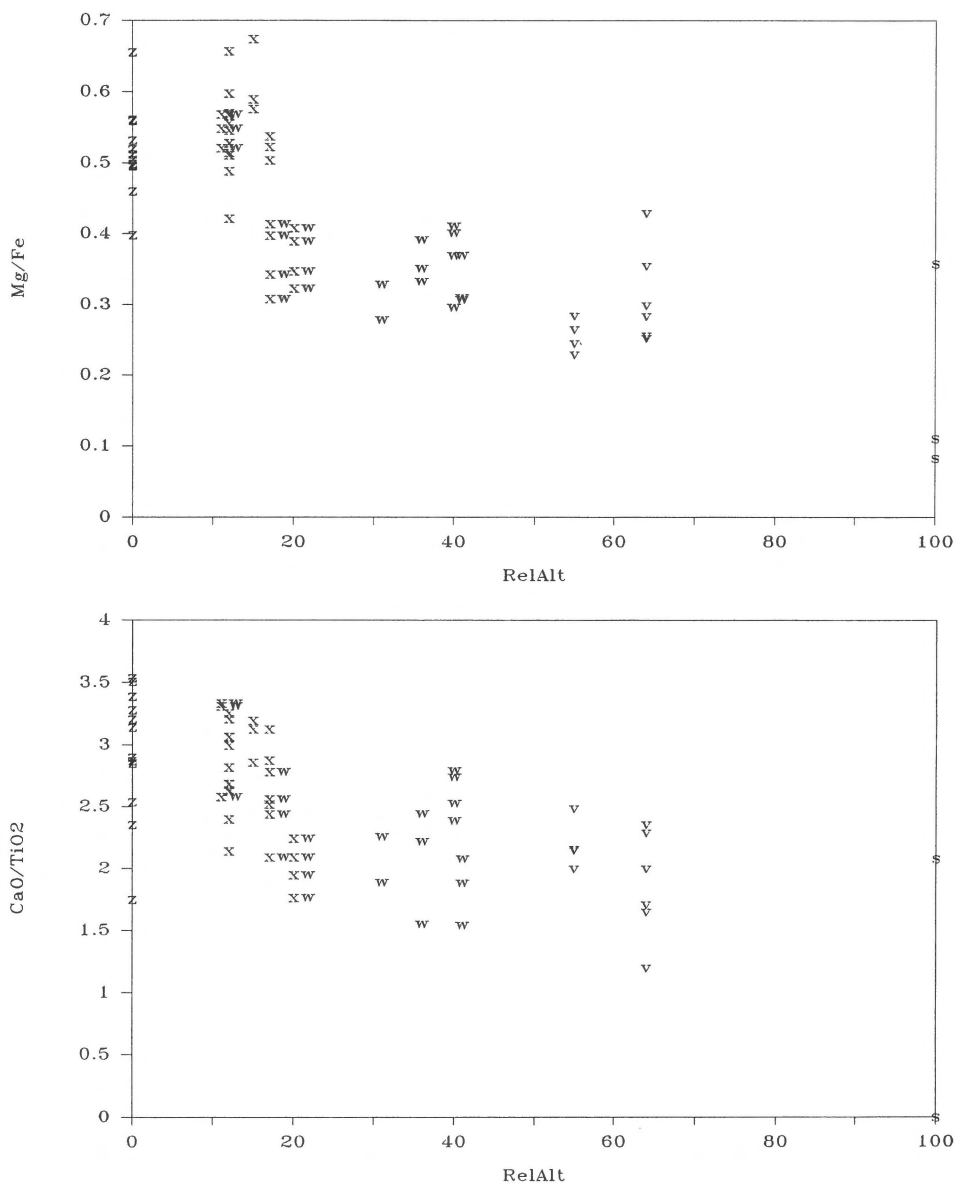


Fig. 9a. Decreasing MgO/Fe<sub>2</sub>O<sub>3</sub> with increasing terrace height indicates progressive weathering. b. Do. for CaO/TiO<sub>2</sub>.

**Variation between terrace levels: long-term changes in sediment supply**

As shown above (Fig. 4, 6), three clusters of sediment composition can be distinguished: one rich in basaltic component (x terrace), one very poor in basaltic components (s), and an intermediate group which comprises both the present river bed z and the xw, w and v terraces. This is concordant

with the much higher content of heavy particles in the x terrace (even over 50%), than in the other terraces (Fig. 10).

The increase of basaltic components going down from the oldest s level to the x level and its subsequent decrease to the present river bed can be explained in several ways:

1. *Tectonics*: Uplift and increasing downcutting of the river may lead to increased admixture of fresh

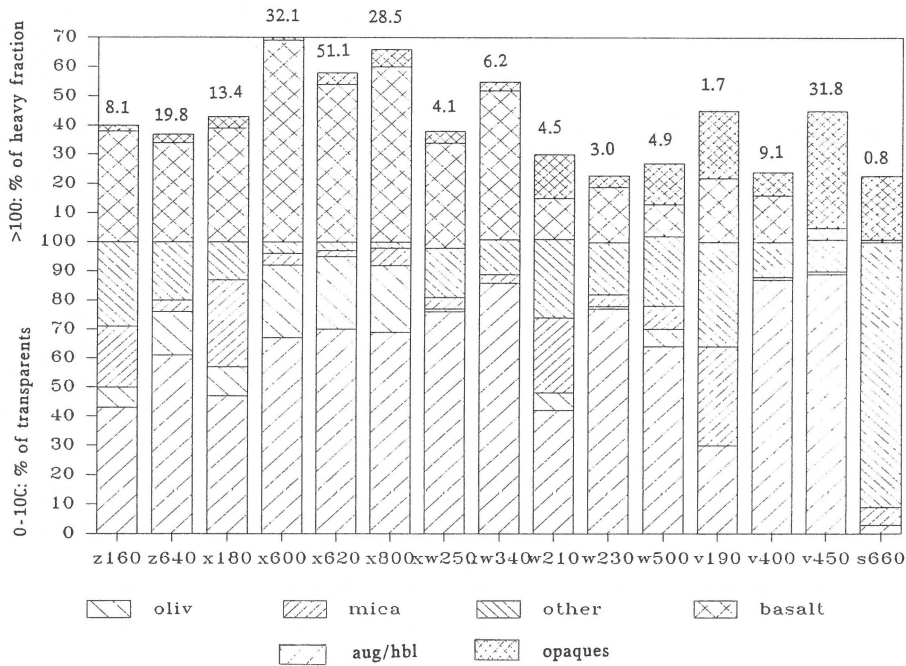


Fig. 10. Heavy mineral composition of samples from different terrace levels: note increase in opaques and decrease in basaltic rock fragments with terrace height as a result of weathering, and increase of mica with decreasing grain size. Numbers above bars indicate percentage of heavy fraction in sample. Terrace symbols and medians below bars.

basaltic rocks to old reworked quartz-rich s-terrace deposits. Such a model exists for instance to explain decreasing quartz contents in gravels of the Meuse and Rhine terrace gravels (Van Straaten, 1946; Brunnacker & Boenigk, 1983). This may explain the basalt-richer composition of the v terrace with respect to the very quartz-rich s terrace. However, further down this effect is probably negligible, as little difference in basalt content exists between the 60 m terrace (v) and the 35 m terrace (w). Moreover, the present river bed z is poorer in basalt than the x terrace (Fig. 6).

2. *Volcanism*: Basaltic volcanism in the headwaters of the Allier has occurred throughout the Pleistocene down to the Early Holocene, and hence fresh basalt flows during the Weichselian may have contributed to the high basalt content of the x terrace. However, it is unlikely that this effect would have dissipated already completely in the Holocene deposits. Moreover, although Late Pleistocene and Holocene volcanism mainly produced scoria cones (Camus et al., 1983), there is very little pyroclastic

material present in the sediments. Most alkalibasaltic particles are non-vesicular, and probably originated from much older basaltic lava flows by granular disintegration during weathering ('coup-de-soleil' structures).

3. *Climatic change*: Upstream from the sector studied here, the Allier river is fed i) by the trunk stream, which drains largely non-glaciated crystalline and basaltic areas, and ii) by the Allagnon and Couze Chambon tributaries, which drain the Cantal and Mont-Dore volcanic massifs. Unpublished data show that the Allagnon sediments are much richer in basalt than the Allier upstream from their confluence. The volcanic massifs were heavily glaciated during the last glacial. It is conceivable, that a large amount of basalt-rich fluvio-glacial sediment was fed by these rivers into the Allier during deglaciation. This is also suggested by the strong increase in volume of x terrace sediments downstream from the confluence (BRGM, 1975). Present-day sediment supply from those tributaries seems much less than that of the trunk stream,

however. Basalt-rich sediments would then correspond to glacial periods, basalt poorer sediments to interglacial periods.

## Conclusion

The geochemistry of bulk samples of the Allier fluvial sands within single terrace levels is mainly controlled by lateral and longitudinal sorting processes, notably by density and shape. The geochemical differences between terrace levels partly reflect uplift and erosion history, partly variations in sediment supply due to climatic changes. The large spread in chemical composition of the Allier terrace sands is largely due to variations in the *amount* of heavy basaltic rock fragments. The large compositional variation remains virtually undetected if only the rather monotonous composition of the transparent heavy minerals is studied. This type of analysis is therefore a useful and rapid analytical tool next to classical sedimentary petrography. Bulk geochemistry of terrace sediment, in conjunction with data on sediment volumes, will be used to model sediment fluxes in glacial and interglacial times under various uplift regimes.

## Acknowledgements

A.J. Kuijper carried out the XRFS analysis; the pre-treatment of samples was carried out by A. Engelsma. Granulometrical analyses have been carried out by the Stichting Technisch Centrum voor de Keramische Industrie, Arnhem. Ir. A. Stein is thanked for his support in statistical matters. The comments on an early version of parts of this report by Drs. P.A. Riezebos are gratefully acknowledged. Dr. W.G. Sombroek is thanked for the use of computing facilities at ISRIC, Wageningen. This research forms part of the project VF LU 86-09, Variability in landscape, soil and vegetation, of the Agricultural University.

## References

- Abbey, S. 1980. Studies in 'Standard samples' for use in the general analysis of silicate rocks and minerals. Part 6: 1979 edition of 'usable' values – Geol. Surv. Canada Pap. 80-14: 30 pp
- Autran, A., & J.M. Peterlongo. 1980. Le Massif Central. – Géologie des Pays Européens – France, Belgique, Luxembourg – Dunod (Paris): 3–133
- Brunnacker, K. & W. Boenigk. 1983. The Rhine Valley between the Neuwied basin and the Lower Rhenish Embayment – In: Fuchs, K. et al. (eds): Plateau Uplift – Springer (Berlin): 62–72
- BRGM. 1975. Val d'Allier. Synthèse des ressources en eau et en granulats dans les Départements du Puy-de-Dôme et de l'Allier – Serv. Géol. Régional Massif Central, Cournon d'Auvergne: 56 pp
- Camus, G., A. de Goër de Herve, G. Kieffer, J. Mergoil & P.M. Vincent. 1983. Volcanologie de la Chaîne des Puys – Parc Naturel Régional Des Volcans, Clermont-Ferrand: 112 pp
- Franzinelli, E. & P.E. Potter. 1983. Petrology, chemistry and texture of modern river sands, Amazon river system – J. Geol. 91: 23–29
- Jeambrun, M., D. Giot, M. Aubert, A. Gachon, J.F. Lenat et al. 1976. Carte Géologique de la France a 1/50.000, Thiers, Note Explicative – BRGM, Orléans: 50 pp
- Kroonenberg, S.B., M.L. Moura & A.T.J. Jonker. 1987a. Major and minor elements geochemistry of Pleistocene alluvial terrace sediments, Limagne rift valley, French Central Massif – 12th Intern. INQUA Conf., Ottawa, Canada (Abstract): 204
- Kroonenberg, S.B., R.M. van den Berg van Saparoea & A.T.J. Jonker. 1987b. Late Glacial and Holocene development of semi-closed basins (thaw lakes?) in the Limagne Rift Valley, French Central Massif – Geol. Mijnbouw 66: 4: 297–311.
- Larue, J.P. 1979. Les nappes alluviales de la Loire et de ses affluents dans le Massif Central et dans le sud du Bassin Parisien: Étude géomorphologique – Thèse Géographie Univ. Clermont II: 543 pp
- Larue, J.P. 1982. Les enseignements climatiques et tectoniques fournis par l'étude des nappes alluviales de la Loire et ses affluents – Rev. Géomorphol. Dyn. 31: 137–149
- Pastre, J.F. 1986. Altération et paléoaltération des minéraux lourds des alluvions pliocènes et pléistocènes du bassin de l'Allier (Massif Central, France) – Assoc. Fr. Étude Quat. Bull. 3/4: 257–269
- Pelletier, H. 1971. Sur les minéraux lourds transparents des alluvions anciennes et récentes de la Limagne d'Auvergne – Thèse Fac. Sci. Clermont-Ferrand: 79 pp
- Raynal J.P. 1984. Chronologie des basses terrasses de l'Allier en Grande Limagne (Puy-de-Dôme, France) – Assoc. Fr. Étude Quat. Bull. 21: 79–84
- Rubey, W.W. 1933. The size-distribution of heavy minerals within a water-laid sandstone – J. Sed. Petr. 3: 3–29
- Rudel, A. 1963. Les minéraux lourds des terrasses quaternaires

- de Limagne d'Auvergne et les éruptions montdoriennes – Soc. Géol. Fr. Bull. (7): 468–469
- Schuiling, R.D., R.J. de Meijer, H.J. Riezebos, M.J. Scholten. 1985. Grain size distribution of different minerals in a sediment as a function of their specific density – Geol Mijnbouw 64: 199–203
- Schumm, S.A., M.P. Mosley & W.E. Weaver. 1987. Experimental fluvial geomorphology – Wiley (New York): 413 pp
- Smith, G.A. & R.D. Smith. 1985. Specific gravity characteristics of recent volcanoclastic sediment: implications for sorting and grain size analysis – J Geol 93: 619–622
- Tourenq, J. 1986. Étude sédimentologique des alluvions de la Loire et de l'Allier, des sources au confluent; les minéraux lourds des roches des bassins versants – Doc. BRGM 108: 108 pp
- Van Andel, Tj.H. 1950. Provenance, transport and deposition of Rhine sediments – Thesis. H. Veenman & Zonen (Wageningen): 129 pp
- Van Dorsser, H.J. 1969. Étude géomorphologique dans une partie de la vallée de l'Allier dans la Grande Limagne – Publ. ITC, Delft, Pays-Bas, Ser. B 50: 66 pp
- Van Straaten, L.M.J.U. 1946. Grindonderzoek in Zuid-Limburg – Proefschrift Univ. Leiden, Ernest van Aelst (Maastricht): 146 pp